Pittsburgh West LiDAR and DEMs used to Create Predictive Models for Hydrologic Flow Nets and Local Land Subsidence

1. Abstract

This paper explores the use of LiDAR and Digital Elevation Models (DEMs) for analyzing land surfaces with respect to hydrologic discharge and land subsidence. Higher resolution 1-meter DEMs from flown LiDAR data are replacing older 30- and 10-meter resolution DEMs, providing more accurate projections. Rasters created from this high-resolution elevation data can be used to create predictive flow models and land subsidence models using GIS. The National Hydrologic Dataset (NHD) and the Soil Survey Geographic Database (SSURGO) are valuable sources of data for both hydrologic discharge and soil taxonomy. Pittsburgh, a city with steep terrains, is surrounded by mountains and receives a decent amount of precipitation, making it a hotbed for landslides. The paper describes methods used to create flow nets, calculate topographic moisture index (TMI), and create a failure index model for areas at high risk of landslides.

2. Introduction

LiDAR and Digital Elevation Models (DEMs) can be used to analyze land surfaces with respect to hydrologic discharge and land subsidence. Older 30- and 10-meter resolution DEMs are systematically being replaced with higher resolution 1-meter DEMs from flown LiDAR data. Plotting data from all three of the resolutions shows the slight variance in elevation differences, with the most accurate projection being LiDAR. With this high-resolution elevation data, it is easier to use rasters to create predictive flow models, as well as land subsidence models using GIS. The National Hydrologic Dataset (NHD), as well as the Soil Survey Geographic Database (SSURGO) offered valuable data for both hydrologic discharge and soil taxonomy for use in calculating drainage nets and land failure models. According to NOAA, Pittsburgh is a city with steep terrains, and is surrounded by mountains; additionally, it receives a decent amount of precipitation, having a 30-year average of 39.61 in/yr. Due to the terrain, geology and amount of precipitation that Pittsburgh receives, it has become a hotbed for landslides. Understanding the amount of water and where it goes, along with soil type and location, predictive surfaces can be calculated for areas which have a high risk of landslides. See the reference map for spatial clarity (fig.1).

3. Methods

3.1 Spatial profile and hillshade analysis

For this work, raster data from the Pennsylvania Spatial Data Access (PASDA) was used. LiDAR (1-meter), 30-meter, and 10-meter DEMs were utilized. The rasters used were imagery obtained over west Pittsburgh. After loading the data into ArcGIS Pro, the tiles were extracted to create equally sized raster tiles based on the LiDAR size. Once the sizes were equalized, the tiles were stacked on top of each other, and a transect was drawn from the northwestern corners to the southeastern corner of the tile stack. This ensured that the profile was uniform across all three DEMs. The transect generated an attribute table which was populated with elevation vs distance data. The 10, 30, and LiDAR data points were all plotted against each other to discern if there were any difference. (fig. 2). A 3-panel figure was also created to compare the three DEM resolutions (fig. 3).

3.2 Flow net analysis

After evaluating the spatial profile, a flow net was created using the LiDAR data. First, the DEM was filled. Next, the flow direction was calculated using the filled DEM. The flow accumulation was then calculated using the previous output.

3.3 National Hydrologic Dataset vs calculated flow net

For this step, the methods remained the same from 3.2, only using NHD data for the same area. Flow line data for west Pittsburgh was downloaded and geoprocessed. Once the flow net was created using the NHD data, it was able to be used for the creation of a topographic moisture index based on NHD data.

3.4 Calculating topographic moisture index (TMI) for the Original and NHD flow nets

A slope map was created from the LiDAR DEM using the "slope" processing tool. Percent slope was used to ensure that the output was tan(β). Using the raster calculator, the TMI was calculated using the following equation:

$$\mathrm{TMI} = \ln\left(\frac{\left(\frac{(flow\ accumulation)}{filled\ slope}\right)}{100}\right)$$

The output raster from this equation gave the TMI values for the LiDAR DEM (fig. 4). The original TMI output was layered over the NHD TMI output for comparison (fig. 5).

3.5 Creating a failure index model

The final part of this lab involved creating the failure index model. First, the relevant data from SSURGO was downloaded. The soil raster was loaded into ArcGIS and extracted to be the same size as the lidar tile. The SSURGO data table was then joined to the SSURGO tile via 'mukey', which is a unique identifier for soil map units within the SSURGO database. This 10-digit code allows the data to be joined with a GIS. Once this join was completed, raster layers were created for the average depth (AVG_THK), hydraulic conductivity (AVG_KSAT) and bulk density (AVG_BD) (fig.6). These rasters were extracted to be the same size as the LiDAR tile. The soil transmissivity in m^2/day was calculated in the raster calculator using the following equation:

$$T = \left((AVG_{THK}) * (AVG_{KSAT}) * 0.000864\right)$$

where 0.000864 is a conversion factor which transforms soil depth and hydraulic conductivity units to soil transmissivity in m^2 per day. The conversion looks like this: ((1/106) / (1/60/60/24) *(1/100)).

After this, the wetness factor (W) was created as its own raster using the following equation:

$$W = \left(\frac{qA}{bTsin\theta}\right)$$

where, 'q' is data derived from 2-year storm data for the area. This data can be obtained from NOAA's national weather service, specifically, the hydrometeorological design studies center. For this model, 2-year, 24-hour data was used. 'A' is the drainage area – this was calculated in part 3.2. T is the transmissivity which was calculated above. B indicates the size of the pixels, so this value was one since all pixels were equally sized. The slope layer was used as 'θ', however the slope needed to be recalculated and converted to radians. Once this raster was created, the 'con' function was used to remove extreme values which were skewing the dataset.

Once the wetness factor was created, the completed failure index was created using the following formula:

$$F = \left(\frac{tan\theta}{tan\varphi}\right)\left(1 - \ W\left(\frac{\rho_w}{\rho_s}\right)\right)^{-1}$$

where, 'tan(θ)' is the local slope, φ is the friction angle, and the ρ's are the bulk density of the water and soil, respectively. W was already calculated from above. Three separate friction angles were used for comparison. The 20° to 40° range is commonly used, so 25°, 35°, and 40° were used as friction angles. These again had to be converted to radians to be used in the equation. Since standard temperature and pressure (STP) was assumed, the bulk density of water was considered to be 1 g/cm^3. The bulk density of the soil was given from the SSURGO data as AVG_BD. New raster layers were then created for all three of the failure angles. A calculation on paper might look something like this:

$$T = (1.542\ m)\left(5 * 10^6\frac{g}{m^3}\right)(0.000864) = \frac{(8.52 * 10^5)m^2}{day}$$

$$W = \frac{(5.97 * 10^{-3}m)(1.51 * 10^8 m^2)}{(1)(8.52 * 10^5 m^2/day)\sin(0.174)} = \ 0.177\ m/day$$

$$F = \left(\frac{\tan(0.174)}{\tan(0.436)}\right)\left(1 - 0.177\frac{m}{day}\left(\frac{\left(\frac{(1 * 10^6)g}{m^3}\right)}{\left(5 * \frac{10^6 g}{m^3}\right)}\right)\ \right)^{-1} = \ 0.39\frac{m}{day}$$

4. Results and discussion

The hillshade outputs from 3.1 helped to visualize the difference in precision across the three different DEMs (see fig.3). As expected, the LiDAR hillshade appeared to be the most precise and the 30-meter data was the least precise (see fig. 3). These hypotheses were confirmed by the plot which was created to compare the transect of the 3 slopes (see fig. 2). While the 30- and 10-meter rasters showed slight variations in their distance to elevation points, the LiDAR show significant differences from both the 10 and 30 meters DEMs – up to 20 meters in certain areas. The 1-meter LiDAR data is much more precise when it comes to capturing small variation in a landscape, so these results were not unexpected. It is recommended to work with LiDAR data if it is available due to its precision. This is why the LiDAR data was used to the rest of the geoprocessing in this lab.

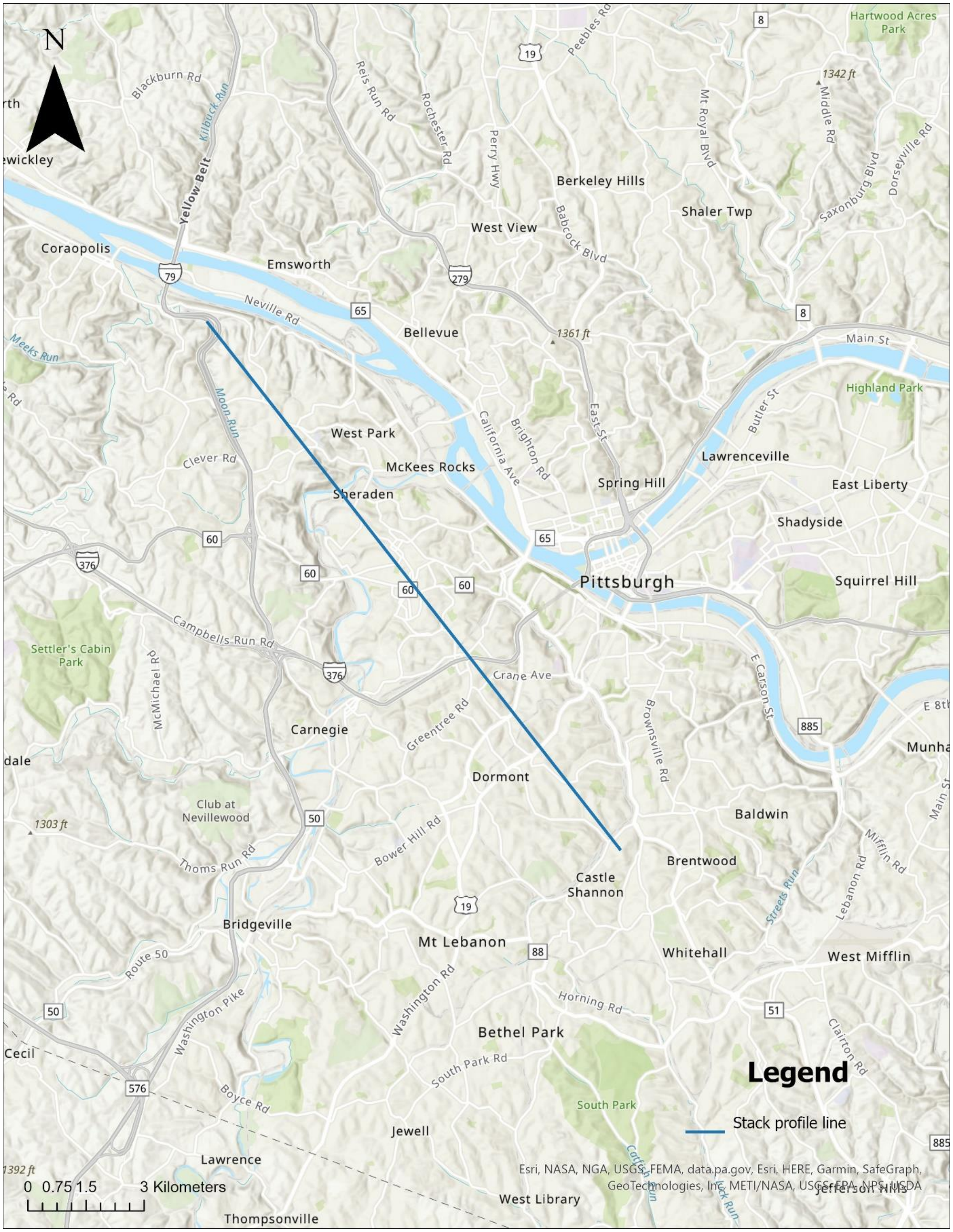

Fig. 1 – Reference map for DEM locations in West Pittsburgh

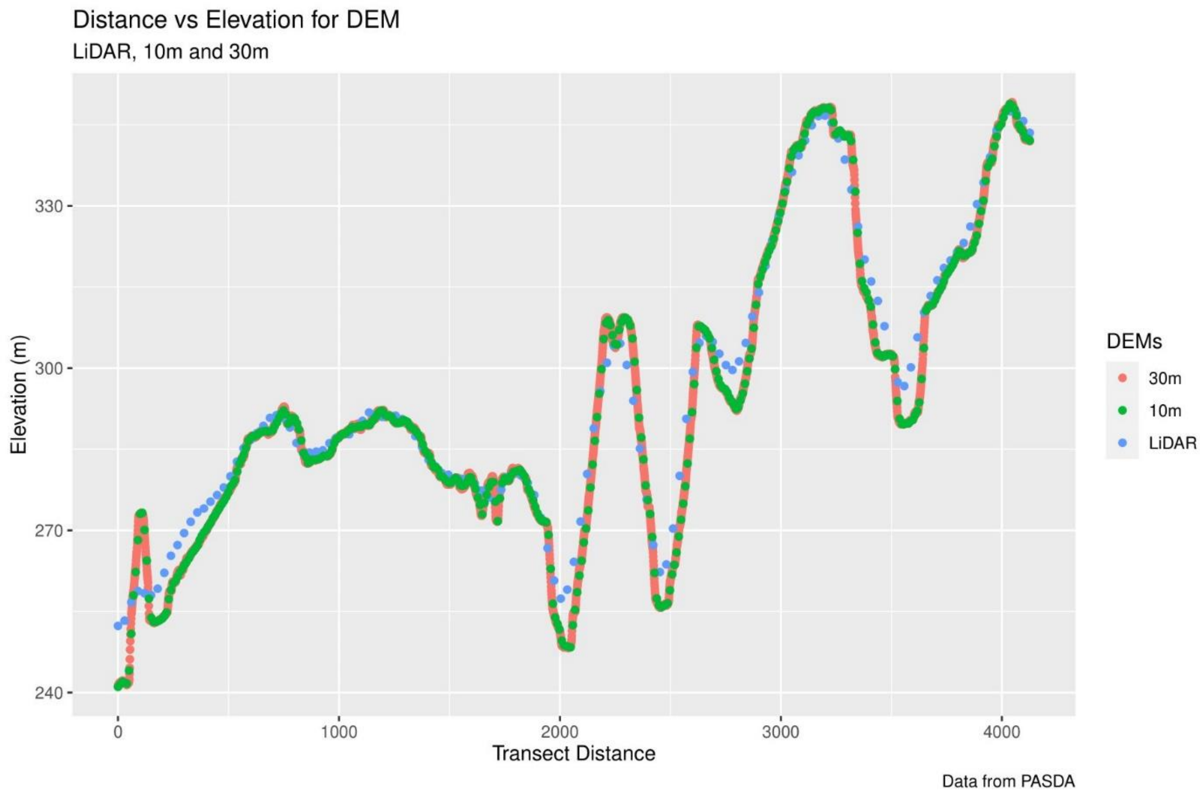

Fig. 2 – Plotted transect data from a combined transect. The LiDAR, 10- and 30-meter data are aligned on top of one another. Discrepancies can be seen as the precision increases with resolution.

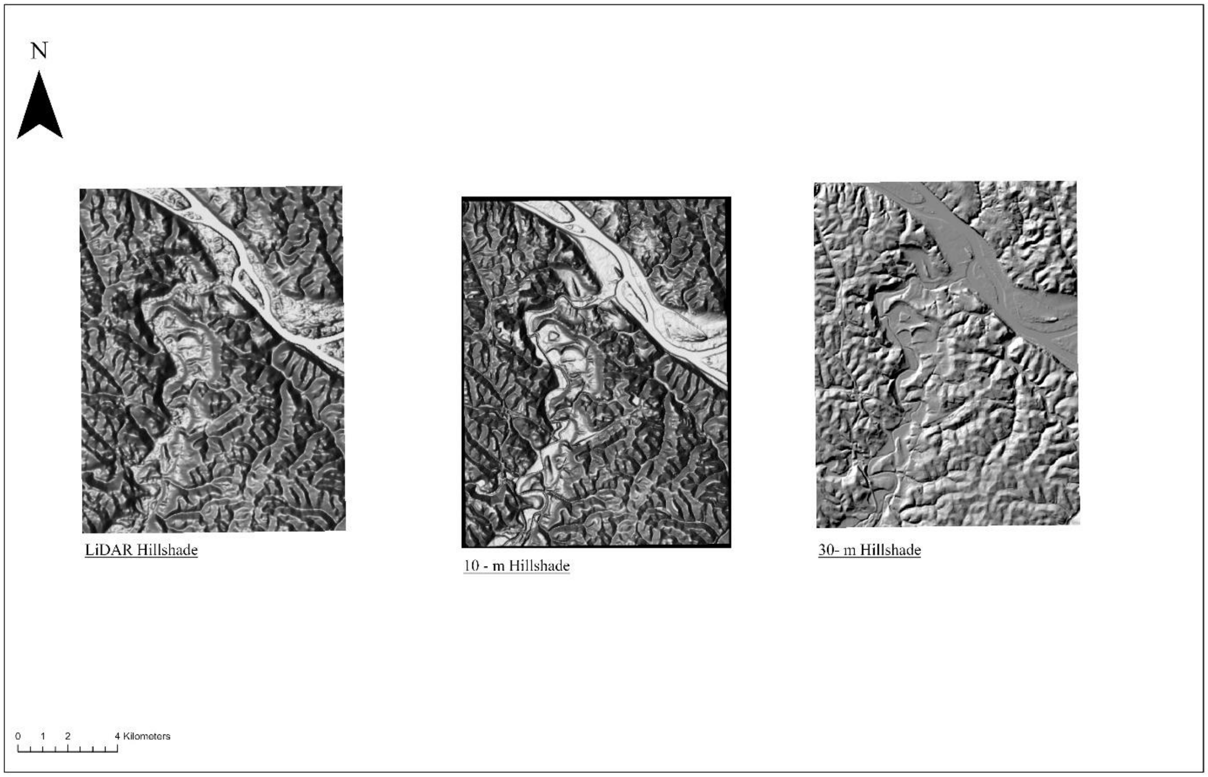

Fig.3 – Three-panel figure showing the different hillshades derived from 1-, 10- and 30-meter digital elevation models.

In part 3.2, the flow directions were calculated using ‘filled’ landscapes. The flows corresponded to a cardinal direction which were represented by different colors. ‘Filling’ the landscape helped to smooth out sinks and peaks in the data using a designated z-value. Outliers and abnormalities are calculated using the surrounding pixels, along with the z-value. Once these are removed, a smoother surface is generated. While this can be a useful tool to ensure the uniformity of the outputs, it can also bias the data. Removing peaks and sinks removes some of the natural variations in the landscape. A plot of a filled vs raw LiDAR tile can be seen below (fig. 7a ,7b). This skews the average slope, which in turn skews the flow lines. The flow accumulation outputs a raster (which is based on the flow direction output) and determines the accumulated flow into each downhill cell. Flow is minimal in most places, which is why this output was mostly black, with few colored pixels. This was true of both the original and NHD outputs.
The TMI was created by taking the natural log of the flow accumulation raster. This creates a much more detailed layer, showing the total wetness in the catchment area. Controls on the flow accumulation and TMI are based off of the actual surface topography, as well as the bulk density of the sediment, hydraulic conductivity and sediment depth. Discharge can also depend on the saturation of the sediments. Soils which have more of a capacity to absorb water (such as a sand) could reduce the flow, whereas an increased percentage of dense, porous substrate, like a clay, could cause increases flow. The SSURGO data supplied classified soil types to each area. This was important to include because of the relationship between hydraulic conductivity, soil permeability and flow.

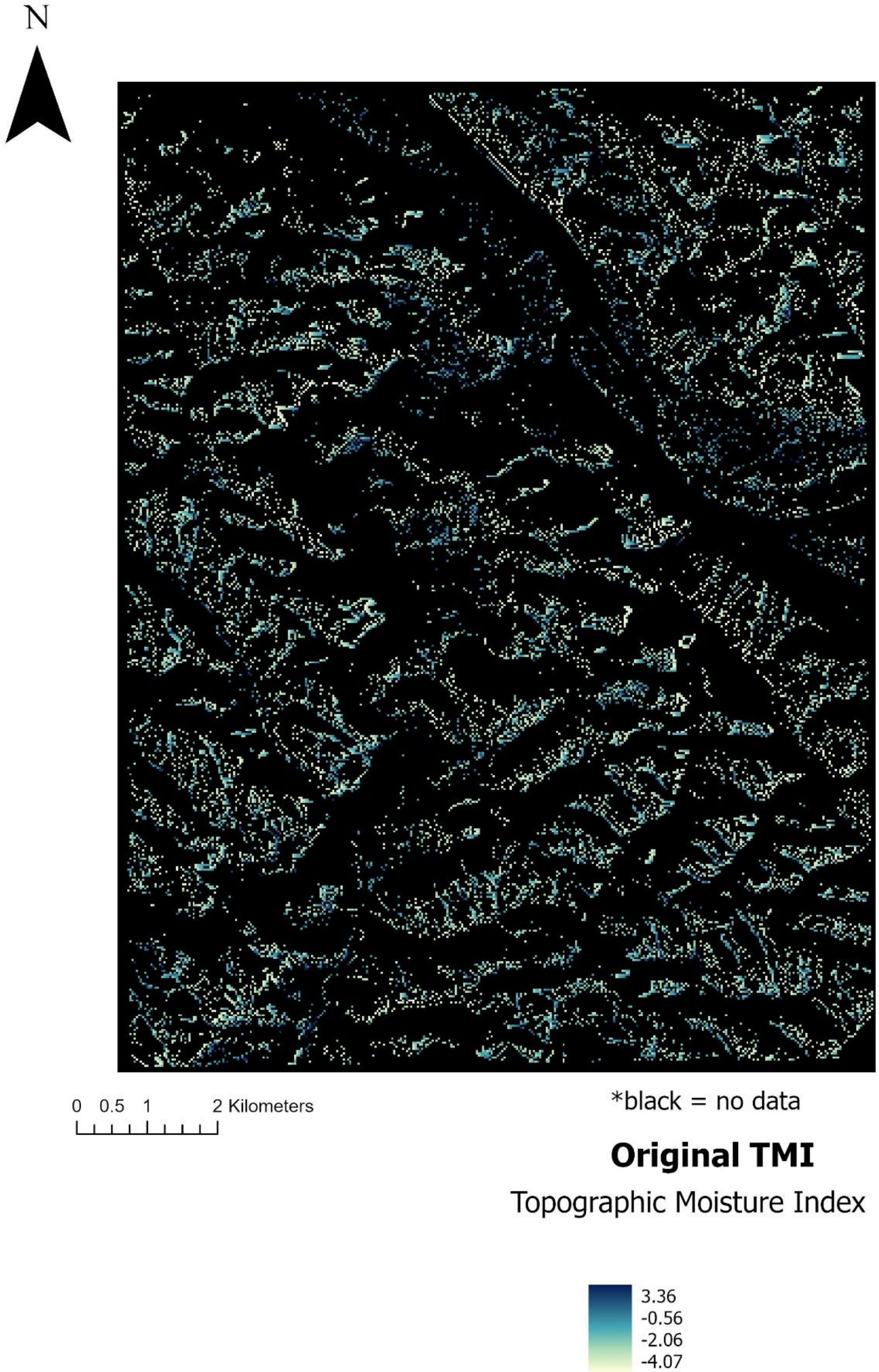

Fig.4 – Original TMI surface before being overlain with the NHD surface.

Fig.5 – The original flow net overlaid with the NHD flow net.

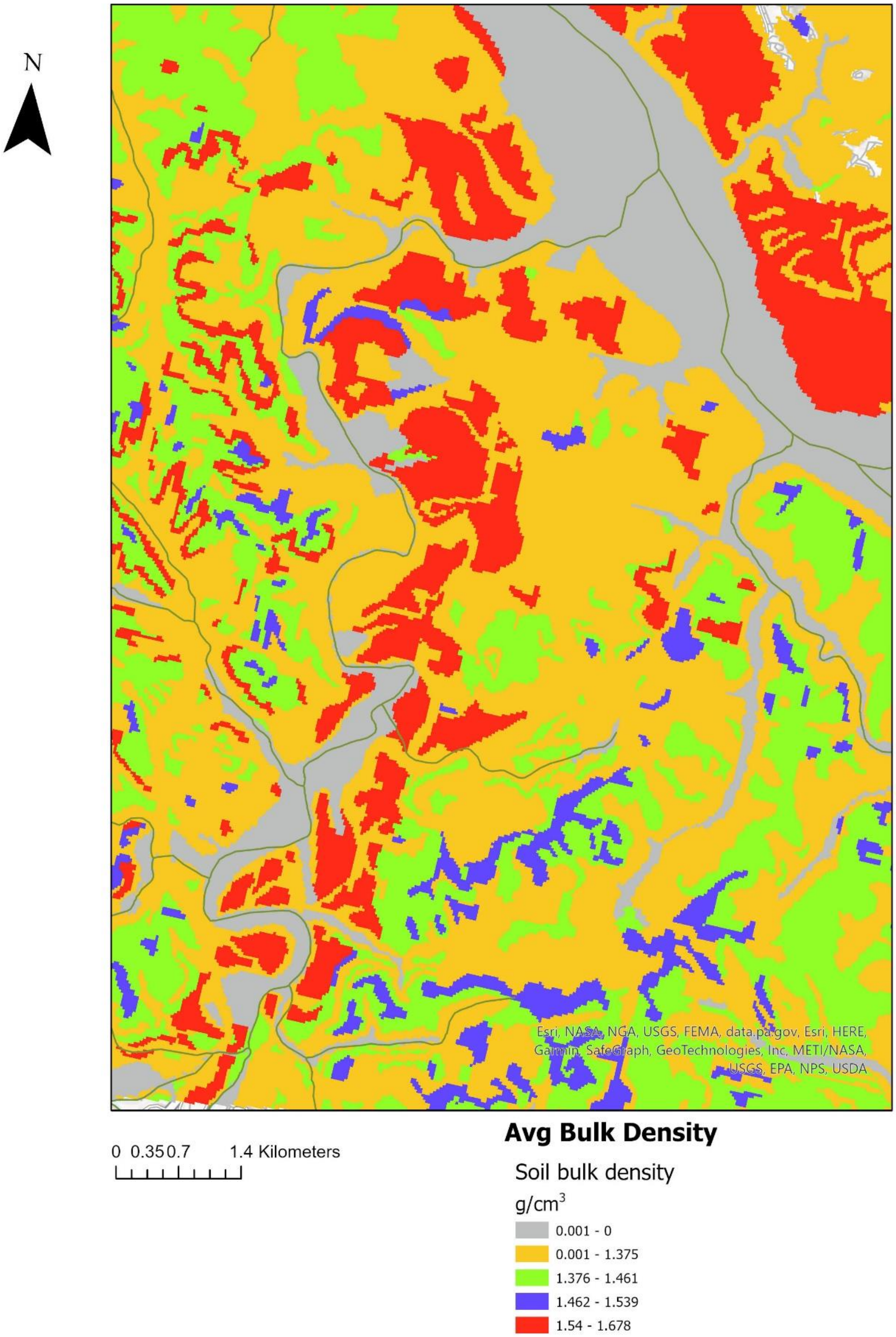

Fig. 6 – Bulk density map using ‘conned’ values from the SSURGO dataset.

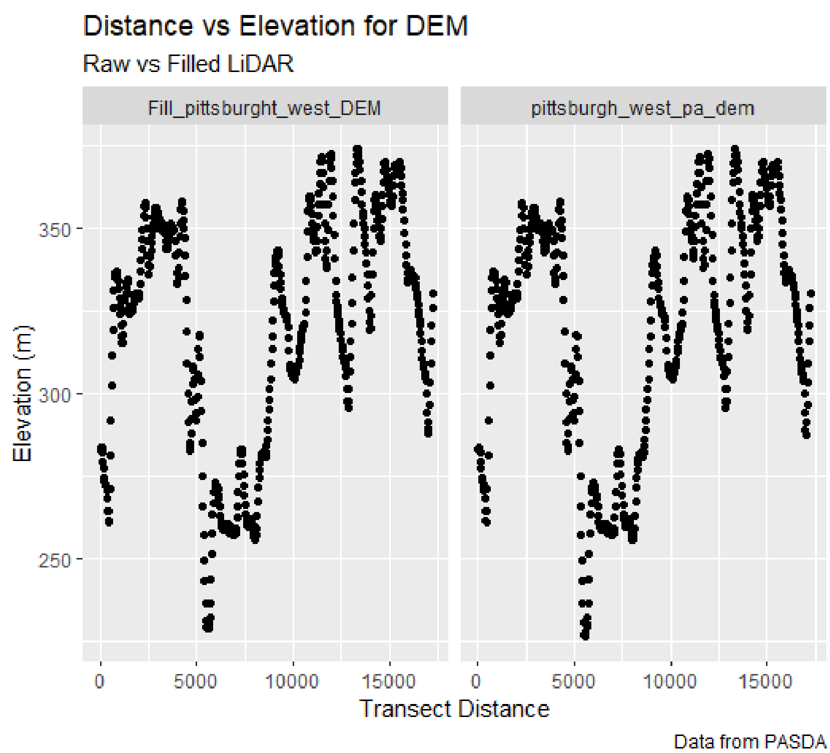

Fig. 7a – A side by side plot for filled vs raw LiDAR data.

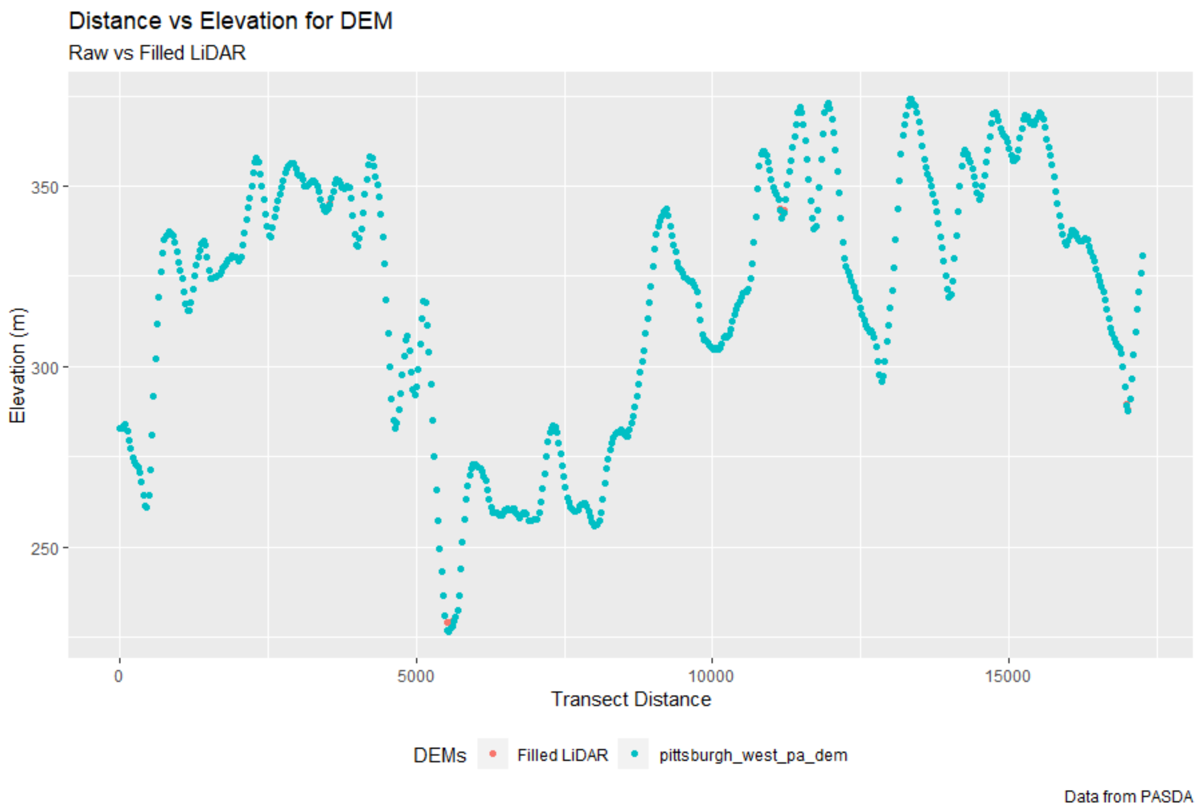

Fig. 7b – Raw LiDAR data plotted on top of filled LiDAR data. Very little variation can be seen from this plot. It is possible that the surface did not need to be statistically adjusted very much due to the lack of outlying peaks and sinks.

The NHD flow net, which was created in the same manner as the original flow net, output a very detailed surface which matched up relatively well with the original TMI surface when overlaid The bias from ‘filling’ was apparent in the relative minima and maxima for each map. NHD data went as high as 12, while the original TMI only went up to around 3.5. Given that this is the same area, it is likely that variations in the z-value created statistical discrepancies in the respective landscapes. By all accounts, the two outputs should have had relatively similar maxima and minima, yet they were off by almost an order of magnitude. The number of pixels for each of the TMI charts were plotted, on a log scale, against a TMI scale for reference (fig 8.).

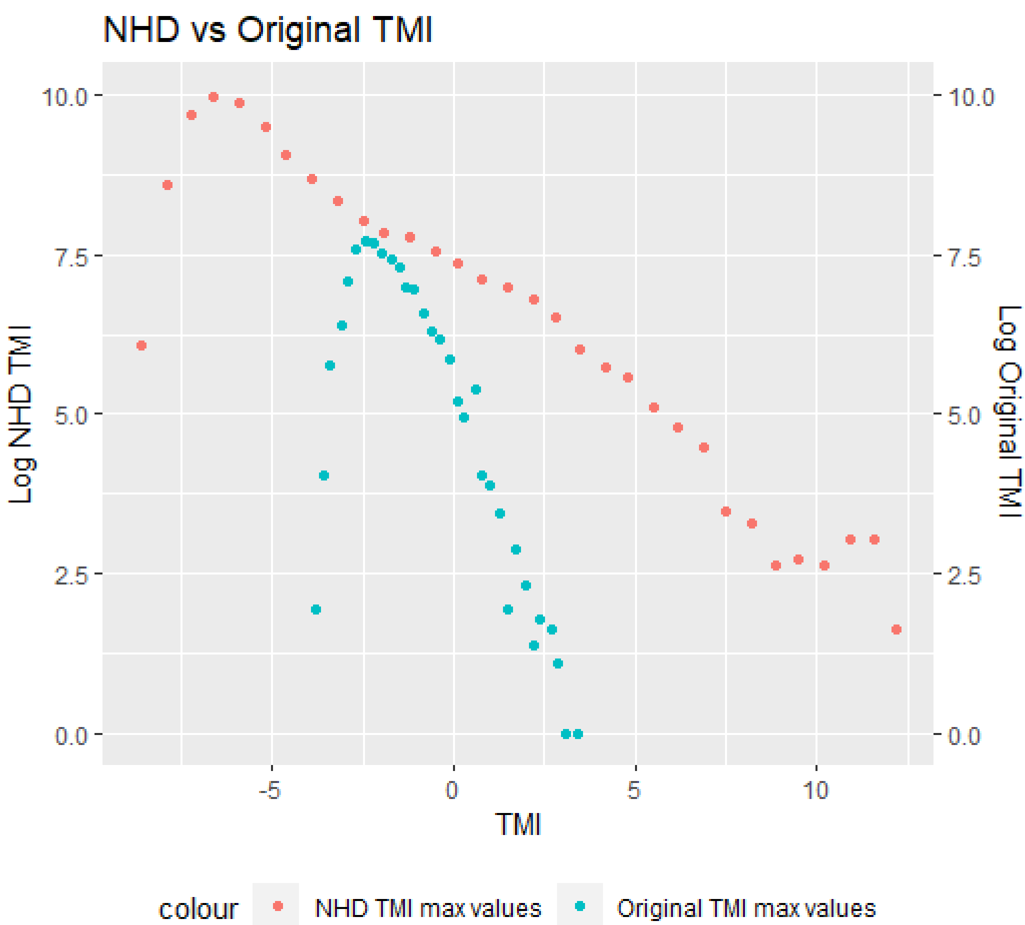

Fig.8 – The distribution of pixels in the TMI plot from both the NHD and original TMI plots. The data has been displayed on a log scale for visual clarity.

The failure indices were created once the hydrologic data had been generated. Three distinct friction angles were used to generate three failure models. Friction angles are the critical angle for sediment on a hillslope. Once this angle is exceeded, the sediment can no longer resist against gravity, causing it to collapse or slide. While these kinds of models can be very useful for creating predictive surfaces, they have some severe limitations. First, friction angles only account for the raw sediment on the hillslope. Many other factors, such as additional support from tree roots and human-caused disruption, can impact sediment collapse. Additionally, these surfaces are stochastic – it is impossible to accurately predict when and where exactly a landslide will occur based on the previous history of the land surface. The spatial distribution of the pixels from all of the failure angles was plotted and can be seen below (fig. 9). Similarly, calculating predictive surfaces with different friction angles can still give an idea of how likely an area is to collapse or slide. As can be seen from the three-panel figure (fig. 10), the likelihood of a slide depends greatly on the friction angle. All other factors being the same, the likelihood of a slide increased greatly in some areas and were non-existent in others when only the friction angle changes. Strangely, the steeper angles generated surfaces which were much less likely to fail, and in fewer areas, than the gentler angles. This can be observed in the three-panel figure (see fig. 10). This was initially unexpected, but upon further examination and research it became clearer. Lower friction angles can indicate that the sediment on the slope has less resistance to the force of gravity, as the steeper angle has to work much harder to fighter against gravity. Additionally, a lower angle can indicate that the sediment or rock is generally weaker in the first place, making it more susceptible to gravity. This creates a cycle of weakening the slope and reducing resistance to gravity even further. The failure areas, in general, corresponded very well to the slope map and to the TMI surfaces. The steepest slopes corresponded directly to the areas which had the largest likelihood of failure in the final failure layers. Additionally, it seemed to be generally true that the wettest areas on the TMI maps also corresponded to the failure maps (it should be noted that this conclusion was drawn only from visuals, not rigorous comparison of the datasets).

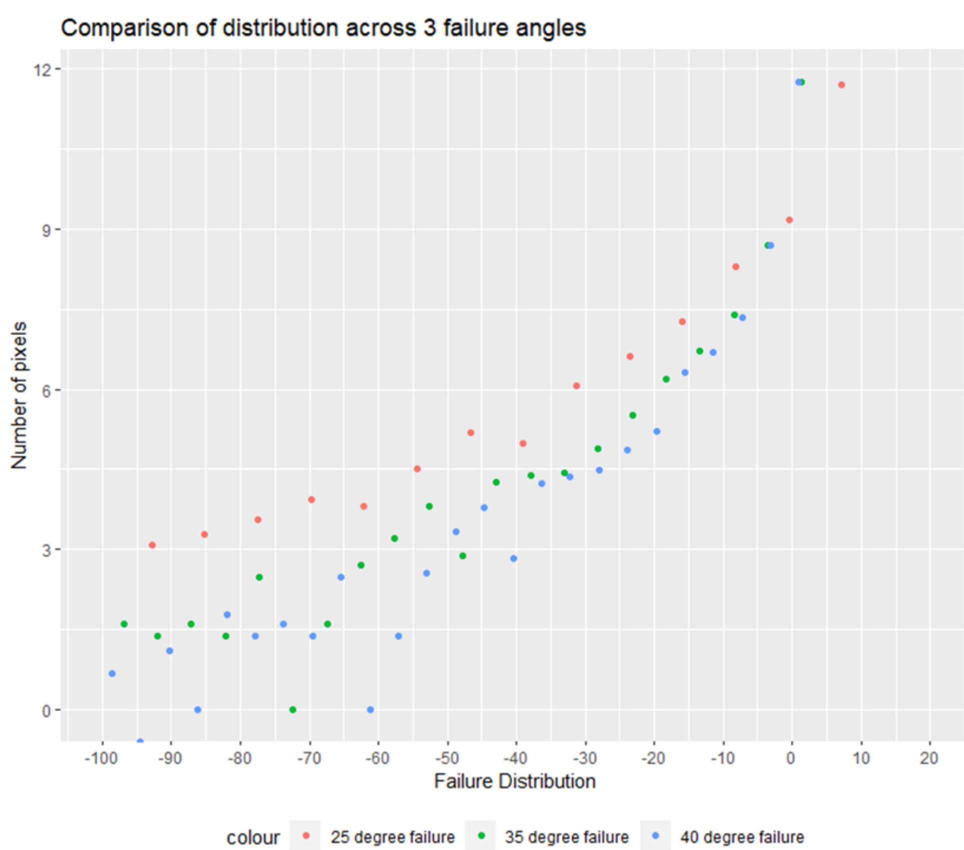

Fig. 9 – All three friction angles vs distribution of pixels based on their value. They all followed a similar curve, with 25° following the cleanest, highest curve.

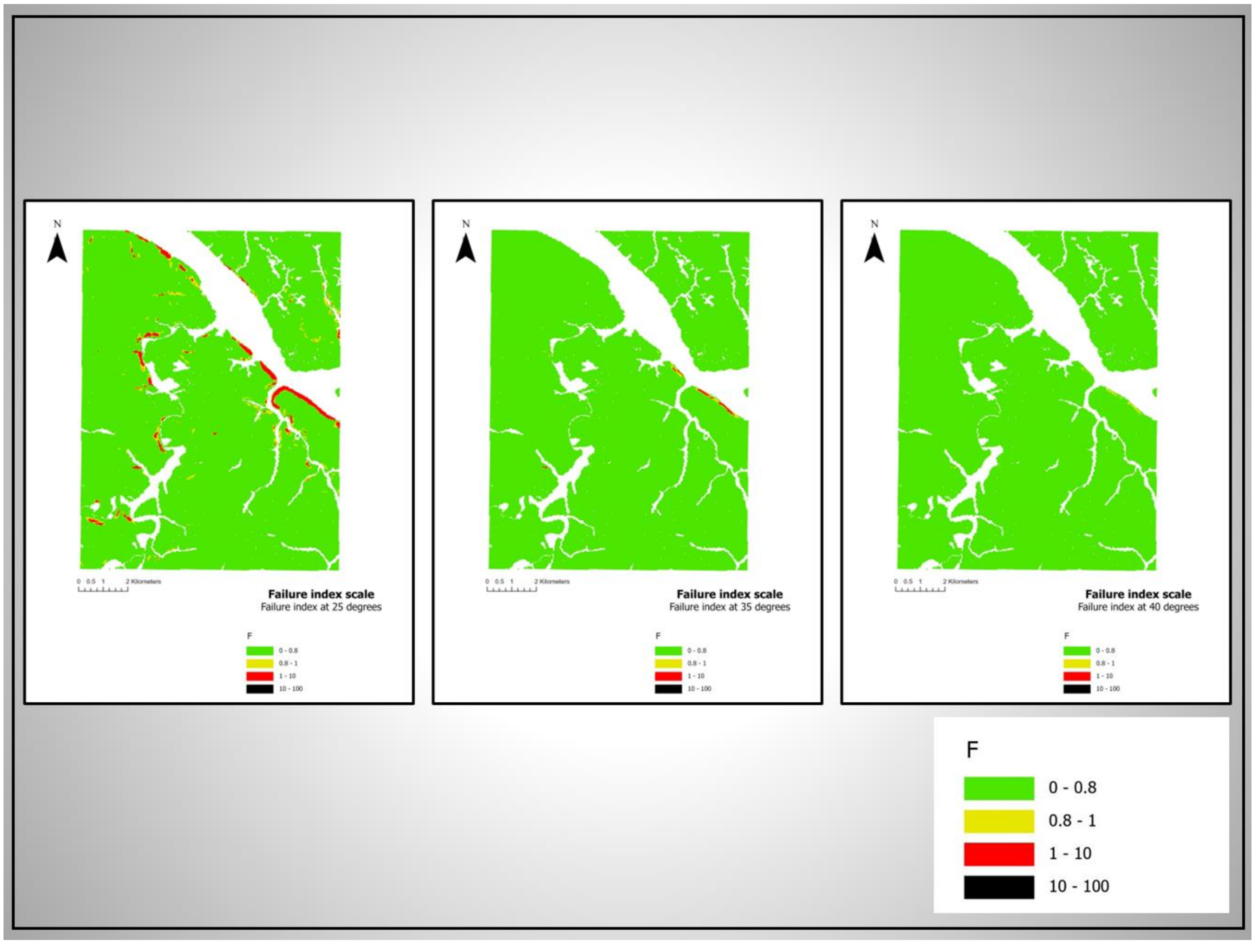

Fig. 10 – A three-panel figure showing the likelihood of land subsidence based on friction angles of 25°, 35°, and 40°. The legend indicated values both below and above 1 in different ranges. Values above 1 indicate higher likelihood of failure.

5. Conclusion

Overall, the use of flow nets to create a failure index can be a very helpful method for understanding changing landscapes and predicting where landslides could be most likely to occur. The limitations of this method included the failure angle not being entirely accurate because of other forces, such as tree roots, acting on the sediment. Additionally, human intervention in landscapes could also greatly impact the likelihood and location of landslides. With the limitations in mind, the friction angle still had a very large impact on each of the predictive surfaces, with the steepest angle having the least likelihood of a landslide, and the lowest angles having the greatest likelihood of landslides, and in more areas. Moreover, the failure surfaces aligned well with both the slope and TMI maps. This indicated that both slope and soil saturation (i.e., hydraulic conductivity) have a large, if not direct impact on the likelihood of a landslide occurring in a given area. (Note: full-sized images of the failure panels will be provided at the bottom of the report for clarity).

6. Works Cited

National Oceanic and Atmospheric Administration. (n.d.). Pittsburgh area hourly precipitation records. Retrieved February 20, 2023, from https://www.weather.gov/media/pbz/records/hisprec.pdf

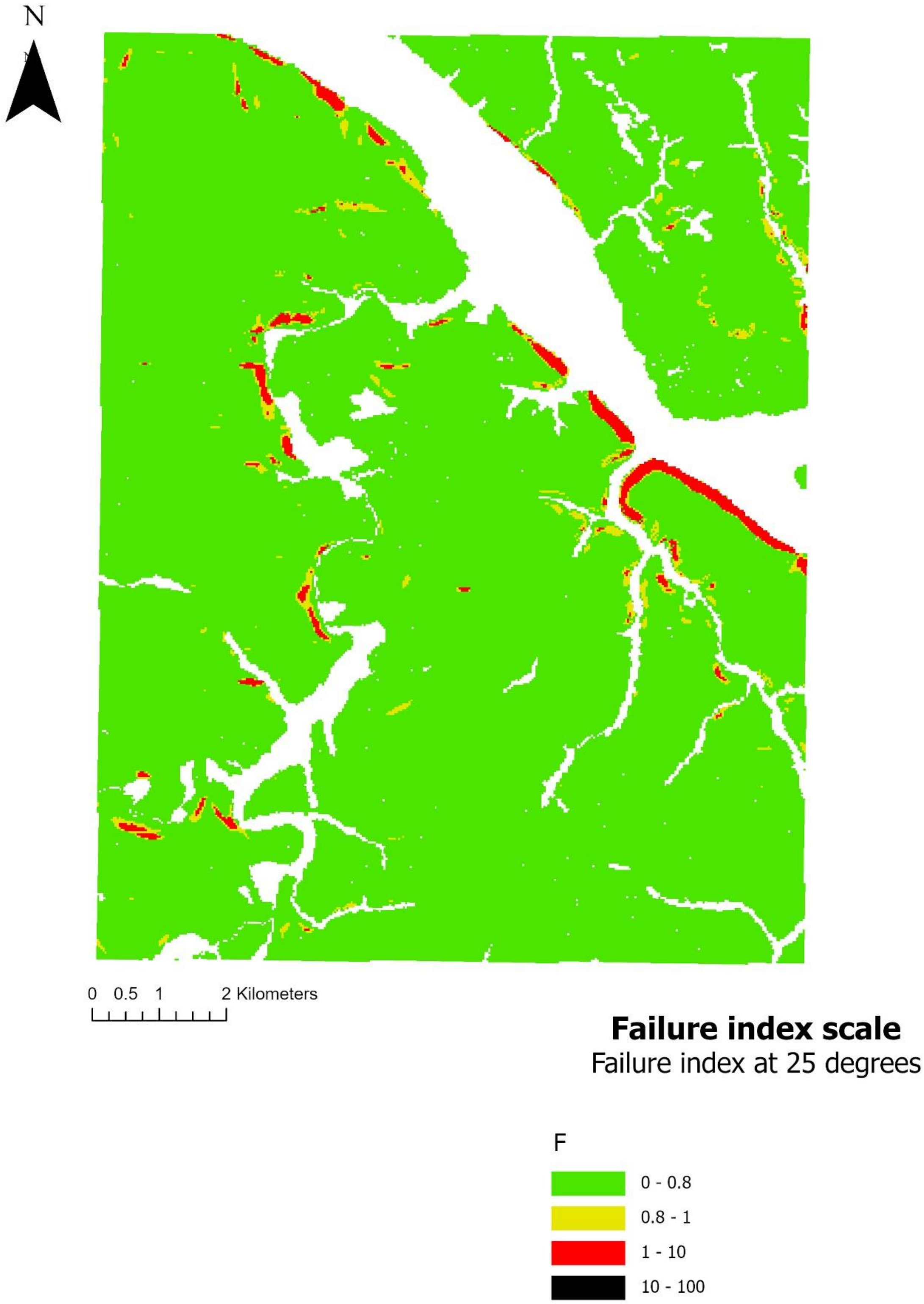
N
0 0.5 1 2 Kilometers
Failure index scale
Failure index at 25 degrees
F
0 - 0.8
0.8 - 1
1 - 10
10 - 100

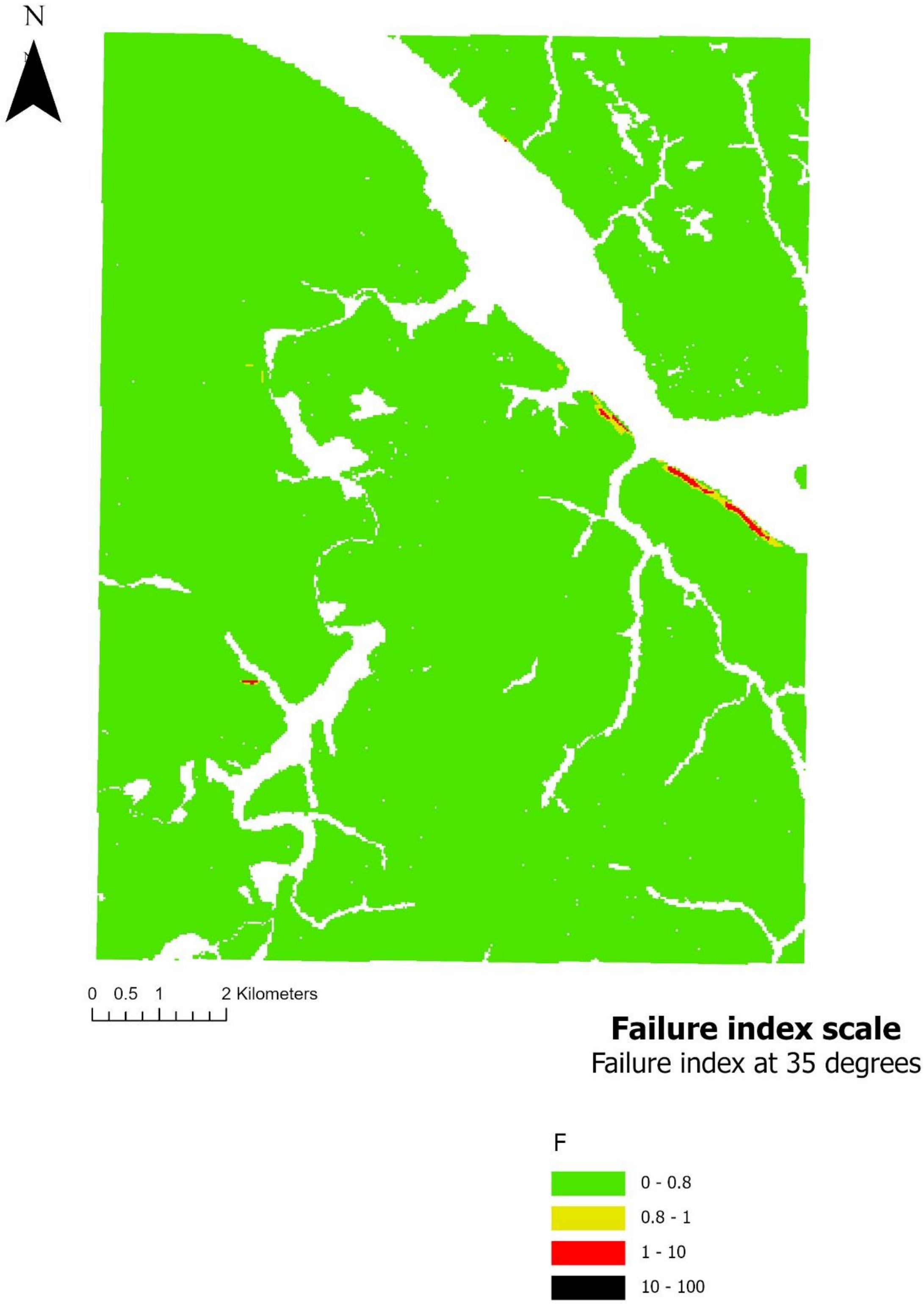
N
0 0.5 1 2 Kilometers
Failure index scale
Failure index at 35 degrees
F
0 - 0.8
0.8 - 1
1 - 10
10 - 100

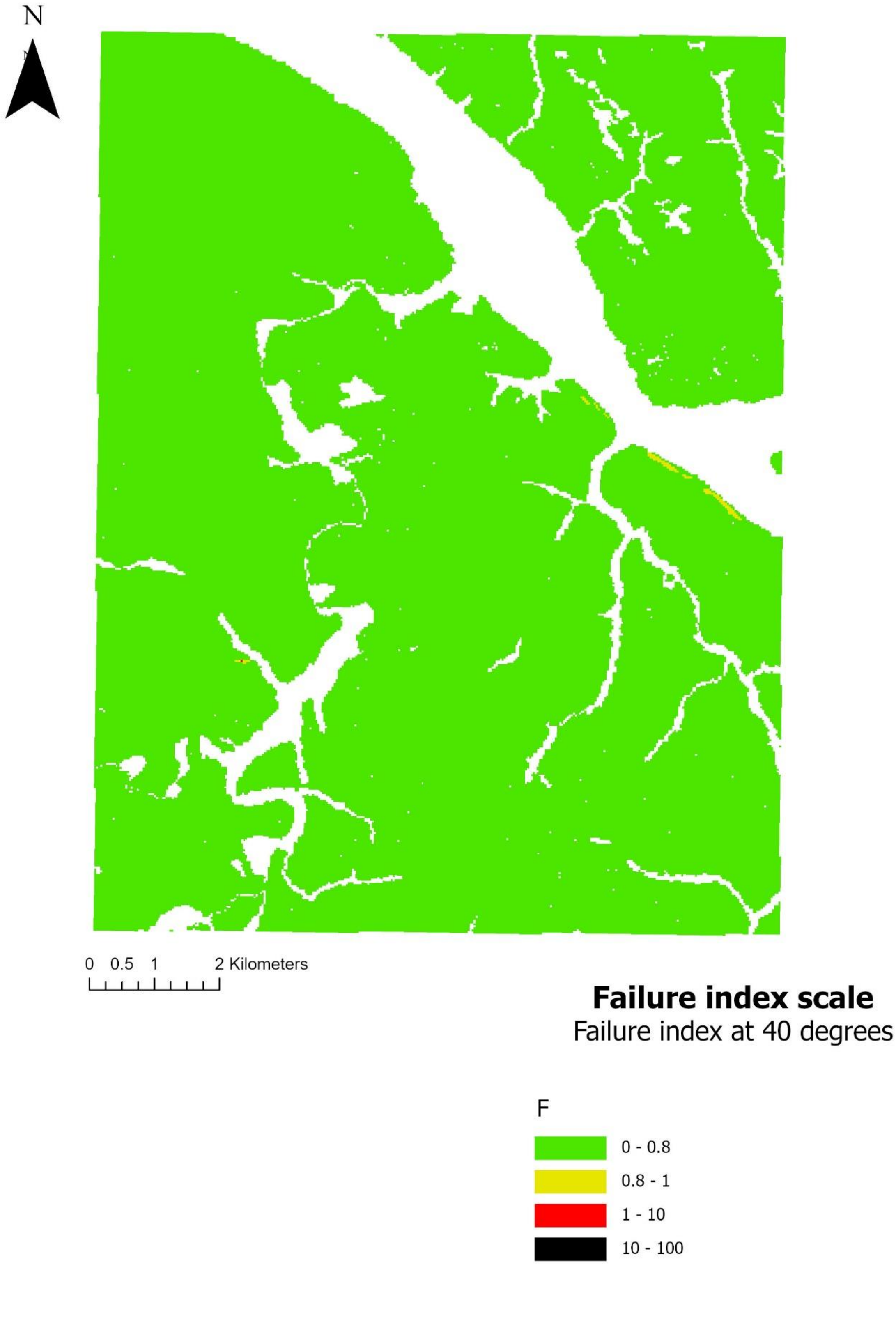
N
0 0.5 1 2 Kilometers
Failure index scale
Failure index at 40 degrees
F
0 - 0.8
0.8 - 1
1 - 10
10 - 100